



Absinthin, an agonist of the bitter taste receptor hTAS2R46, uncovers an ER-to-mitochondria Ca^{2+} –shuttling event

Received for publication, January 27, 2019, and in revised form, June 17, 2019. Published, Papers in Press, June 27, 2019; DOI 10.1074/jbc.RA119.007763

Maria Talmon^{†1}, Silvia Rossi^{†1}, Dmitry Lim[§], Federica Pollastro[§], Gioele Palattella[‡], Federico A. Ruffinatti[§], Patrizia Marotta[§], Renzo Boldorini[‡], Armando A. Genazzani^{§2}, and Luigia G. Fresu^{‡3}

From the [‡]Department of Health Sciences, School of Medicine, University of Piemonte Orientale, Via Solaroli, 17-28100 Novara, Italy and [§]Department of Pharmaceutical Sciences, University of Piemonte Orientale, Via Bovio, 6-28100 Novara, Italy

Edited by Roger J. Colbran

Type 2 taste receptors (TAS2R) are G protein–coupled receptors first described in the gustatory system, but have also been shown to have extraoral localizations, including airway smooth muscle (ASM) cells, in which TAS2R have been reported to induce relaxation. TAS2R46 is an unexplored subtype that responds to its highly specific agonist absinthin. Here, we first demonstrate that, unlike other bitter-taste receptor agonists, absinthin alone (1 μM) in ASM cells does not induce Ca^{2+} signals but reduces histamine-induced cytosolic Ca^{2+} increases. To investigate this mechanism, we introduced into ASM cells aequorin-based Ca^{2+} probes targeted to the cytosol, subplasma membrane domain, or the mitochondrial matrix. We show that absinthin reduces cytosolic histamine-induced Ca^{2+} rises and simultaneously increases Ca^{2+} influx into mitochondria. We found that this effect is inhibited by the potent human TAS2R46 (hTAS2R46) antagonist 3 β -hydroxydihydrocostunolide and is no longer evident in hTAS2R46-silenced ASM cells, indicating that it is hTAS2R46-dependent. Furthermore, these changes were sensitive to the mitochondrial uncoupler carbonyl cyanide *p*-(trifluoromethoxy)phenyl-hydrazone (FCCP); the mitochondrial calcium uniporter inhibitor KB-R7943 (carbamimidothioic acid); the cytoskeletal disrupter latrunculin; and an inhibitor of the exchange protein directly activated by cAMP (EPAC), ESI-09. Similarly, the β_2 agonist salbutamol also could induce Ca^{2+} shuttling from cytoplasm to mitochondria, suggesting that this new mechanism might be generalizable. Moreover, forskolin and an EPAC activator mimicked this effect in HeLa cells. Our findings support the hypothesis that plasma membrane receptors can positively regulate mitochondrial Ca^{2+} uptake, adding a further facet to the ability of cells to encode complex Ca^{2+} signals.

The existence of a family of bitter taste receptors was predicted over 20 years ago by Lush (1), and bitter taste receptor (TAS2R) genes were first described in 2000 (2). In humans, there are 25 subtypes of G protein–coupled receptors referred

to as hTAS2Rs⁴ (3–5) that vary in their selectivity toward bitter compounds: Some subtypes recognize few chemically restricted molecules, whereas some others respond to a wide range of diverse ligands (6). In the same way, some bitter compounds are known to be agonists for a single hTAS2R subtype, whereas others are not selective (7).

Recently, hTAS2Rs have been reported to be expressed, alongside tongue and palate epithelia, also on extraoral tissues such as gut, genitourinary system, brain, immune cells, and respiratory system (8, 9). In airway smooth muscle (ASM), agonists of the most-represented bitter taste receptor subtypes (TAS2R10, 14, and 31) have been identified as novel pharmacological targets in obstructive pulmonary disease therapy (10–14). The expression of TAS2R and the bronchodilatory effect of the agonists have been confirmed in mouse (15), guinea pig (16), and human (12, 17, 18). Paradoxically, the bronchodilation mechanism induced by activation of TAS2R10, 14, and 31 in response to a contractile stimulus is mediated by an increase in cytosolic calcium followed by membrane hyperpolarization through large-conductance potassium channels (BK_{Ca}) (11, 16). Interestingly, it has been demonstrated that the level of calcium increase is correlated to the level of receptor expression (11). More recently, Tan and Sanderson (19) have found that agonists of TAS2R10, at concentrations required to dilate mouse constricted airways, do not increase cytosolic calcium in ASM, leading to the hypothesis that TAS2R agonists bronchodilate by inhibiting IP_3 receptors and reducing calcium sensitivity.

In the present manuscript, we focused on hTAS2R46, an unexplored hTAS2R subtype receptor in ASM (13). An extensive structure-function analysis of this subtype has been performed (20) and sesquiterpene lactones, such as absinthin, represent selective agonists (6, 21).

We now report that absinthin *per se* does not induce Ca^{2+} rises but significantly reduces the cytosolic Ca^{2+} rise induced by histamine in ASM. This reduction is not a consequence of

This work was supported by Regione Piemonte Grant on Autoimmunity and Allergic Diseases D.D. n.195 18/07/2014 (to L. G. F.). The authors declare that they have no conflicts of interest with the contents of this article.

This article contains supporting Experimental procedures and Figs. S1–S6.

¹ These authors contributed equally to this work.

² To whom correspondence should be addressed. Tel.: 39-0321-375827; Fax: 39-0321-375821; E-mail: armando.genazzani@uniupo.it.

³ To whom correspondence may be addressed. Tel.: 39-0321-660687; Fax: 39-0321-620421; E-mail: luigia.fresu@med.uniupo.it.

⁴ The abbreviations used are: hTAS2R, human type 2 taste receptors; 3HDC, 3 β -hydroxydihydrocostunolide; ANOVA, analysis of variance; ASM, airway smooth muscle; cytAEQ, cytosolic aequorin; EPAC, exchange factor directly activated by cAMP; ER, endoplasmic reticulum; FCCP, carbonyl cyanide *p*-(trifluoromethoxy)phenyl-hydrazone; IP_3 , inositol 1,4,5-trisphosphate; KB-R7943, carbamimidothioic acid; KRB, Krebs-Ringer buffer; LV, lentiviral vectors; sMCU, mitochondrial calcium uniporter; mitAEQ, mitochondrial aequorin; pmAEQ, subplasmalemmal aequorin; tBHQ, 2,5-di-*tert*-butyl-1,4-benzohydroquinone; VDAC, voltage-dependent anion channel.

reduced influx through the plasma membrane nor of a decrease in Ca^{2+} efflux from the endoplasmic reticulum, but is a consequence of an increased Ca^{2+} uptake by mitochondria. Indeed, cytosolic Ca^{2+} decreases and simultaneous mitochondrial Ca^{2+} increases were sensitive to the nonspecific mitochondrial calcium uptake inhibitor carbamimidiothioic acid (KB-R7943), to the mitochondrial uncoupler carbonyl cyanide *p*-trifluoromethoxyphenyl-hydrazone (FCCP), to the selective hTAS2R46 inhibitor β 3-hydroxydihydrocostunolide (3HDC) (7), to the cytoskeletal disrupter latrunculin, and to the EPAC antagonist ESI-09. Furthermore, the effect of absinthin was no longer evident in hTAS2R46-silenced cells. Our observation that absinthin, activating hTAS2R46, modulates histamine-induced cytosol Ca^{2+} rises by potentiating mitochondrial Ca^{2+} uptake shows that regulated mitochondrial Ca^{2+} uptake may participate in the encoding of Ca^{2+} signals. We also provide data that this ER-to-mitochondria shuttling may be a general feature of Ca^{2+} signaling as salbutamol, a β_2 -agonist, also reduces histamine-induced Ca^{2+} rises in the cytosol while simultaneously increasing mitochondrial calcium.

Results

Absinthin reduces histamine-induced Ca^{2+} increases via hTAS2R46

First, we evaluated the effect of absinthin on Ca^{2+} rises in ASM. Although other bitter taste receptor ligands have been shown to increase cytosolic Ca^{2+} (11), absinthin (10 μM) was unable to induce any Ca^{2+} rise ($n = 7$) (Fig. 1A).

We next evaluated the effect of absinthin on the Ca^{2+} -rise induced by one of the most potent bronchoconstrictors, histamine (10 μM). As shown in Fig. 1, A and B, histamine induced a rapid Ca^{2+} rise, as determined by Fura-2. The simultaneous co-addition of absinthin, surprisingly, led to a significantly lower histamine-induced Ca^{2+} peak. This effect was evident when pooling the data together but was just as evident at the single cell level in fluorescence microscopy (data not shown). Because histamine-induced Ca^{2+} rises are the result of an initial Ca^{2+} release from intracellular stores and a secondary Ca^{2+} entry, we performed experiments in a Ca^{2+} -free extracellular buffer to dissect the two components. As demonstrated in Fig. 1B, histamine induced a cytosolic Ca^{2+} rise in this condition, which was of lower amplitude compared with the previous condition. Yet, absinthin was still able to significantly reduce the effect of histamine.

Absinthin is reported to bind different bitter taste receptor subtypes, although it is generally thought to act mainly on hTAS2R46 (6). We therefore evaluated whether hTAS2R46 was present in our cellular model. Indeed, RT-PCR experiments showed that mRNA coding for this subtype was present in ASM, although at lower levels compared with human bronchial muscle and human epithelial tongue (Fig. S1A). This was confirmed also by Western blotting, immunofluorescence, and immunohistochemistry of ASM with specific antibodies (Fig. S1, B–F). We next evaluated whether 3HDC, a potent antagonist of hTAS2R46 (7), was able to revert the effect of absinthin on histamine-induced Ca^{2+} rises. As shown in Fig. 1C, 3HDC

dose-dependently reverted the effect of absinthin, with concentrations of 10 μM abolishing completely the effect of the agonist. To further determine the specificity of this effect, we performed experiments in HeLa cells that are devoid of hTAS2R46 (Fig. S1B) but that have phospholipase C-coupled histamine receptors (22). As shown in Fig. 1D, absinthin was unable to affect histamine-induced Ca^{2+} rises in HeLa cells, even at high concentrations (100 μM). Last, we made use of shRNA to confirm that it was indeed hTAS2R46 mediating the absinthin response. The use of shRNA led to a decrease of the mRNA encoding for the receptor in ASM cells of $90 \pm 2.5\%$ (as determined by RT-PCR and Western blotting) compared with control ASM cells (Fig. S1, A and B). In cells with a significantly reduced level of hTAS2R46, absinthin was unable to reduce histamine-induced cytosolic Ca^{2+} rises (Fig. 1E).

These data demonstrated that absinthin reduced cytosolic Ca^{2+} -rises induced by histamine by a receptor-specific mechanism mediated by hTAS2R46. This effect occurs rapidly and appears to affect the Ca^{2+} -release component of the rise, given that it is apparent also in Ca^{2+} -free conditions.

Absinthin does not affect subplasmalemmal Ca^{2+}

To evaluate whether the Ca^{2+} -entry component of the histamine-induced Ca^{2+} rise was also affected, we decided to use aequorin-based probes that can be targeted selectively to subcellular compartments. At first, we confirmed the effect of absinthin on histamine-induced Ca^{2+} rises using a non-targeted cytosolic aequorin (cytAEQ) (23). In accordance with what was observed with Fura-2, absinthin dampened the peak of the Ca^{2+} rise in a significant manner (Fig. 2A). We next decided to evaluate whether Ca^{2+} entry was affected by using an aequorin probe directed to the subplasma membrane compartment (pmAEQ) (24, 25). In this instance, histamine-induced Ca^{2+} entry was not affected by the co-addition of absinthin (Fig. 2B).

To further confirm that Ca^{2+} entry was not involved, we performed a store depletion experiment investigating cytosolic calcium via Fura-2. Stores were depleted with *t*BHQ (50 μM) in a calcium-free solution and calcium was re-added after 5 min in the presence or absence of absinthin. As shown in Fig. S2, absinthin was unable to affect the extent of store-operated Ca^{2+} entry. These data therefore suggest that absinthin targets selectively the intracellular store component of histamine-induced Ca^{2+} rises.

Absinthin controls mitochondrial calcium buffering

To reconcile the above, partly contradictory observations on absinthin (*i.e.* a decreased cytosolic calcium rise together with an unchanged Ca^{2+} entry), we inquired whether mitochondrial Ca^{2+} in response to histamine would change in accord to cytosolic Ca^{2+} . If absinthin dampens Ca^{2+} release via IP_3R modulation or via IP_3 production, it would be expected that mitochondrial Ca^{2+} uptake in the presence of absinthin after stimulation with histamine should be lowered as well. To test this hypothesis, we used an aequorin probe that targets selectively the mitochondrial matrix (mitAEQ) (24, 26). As shown in Fig. 3A, stimulation of cells with histamine provoked an increase in mitochondrial Ca^{2+}

hTAS2R46 regulates mitochondrial calcium buffering

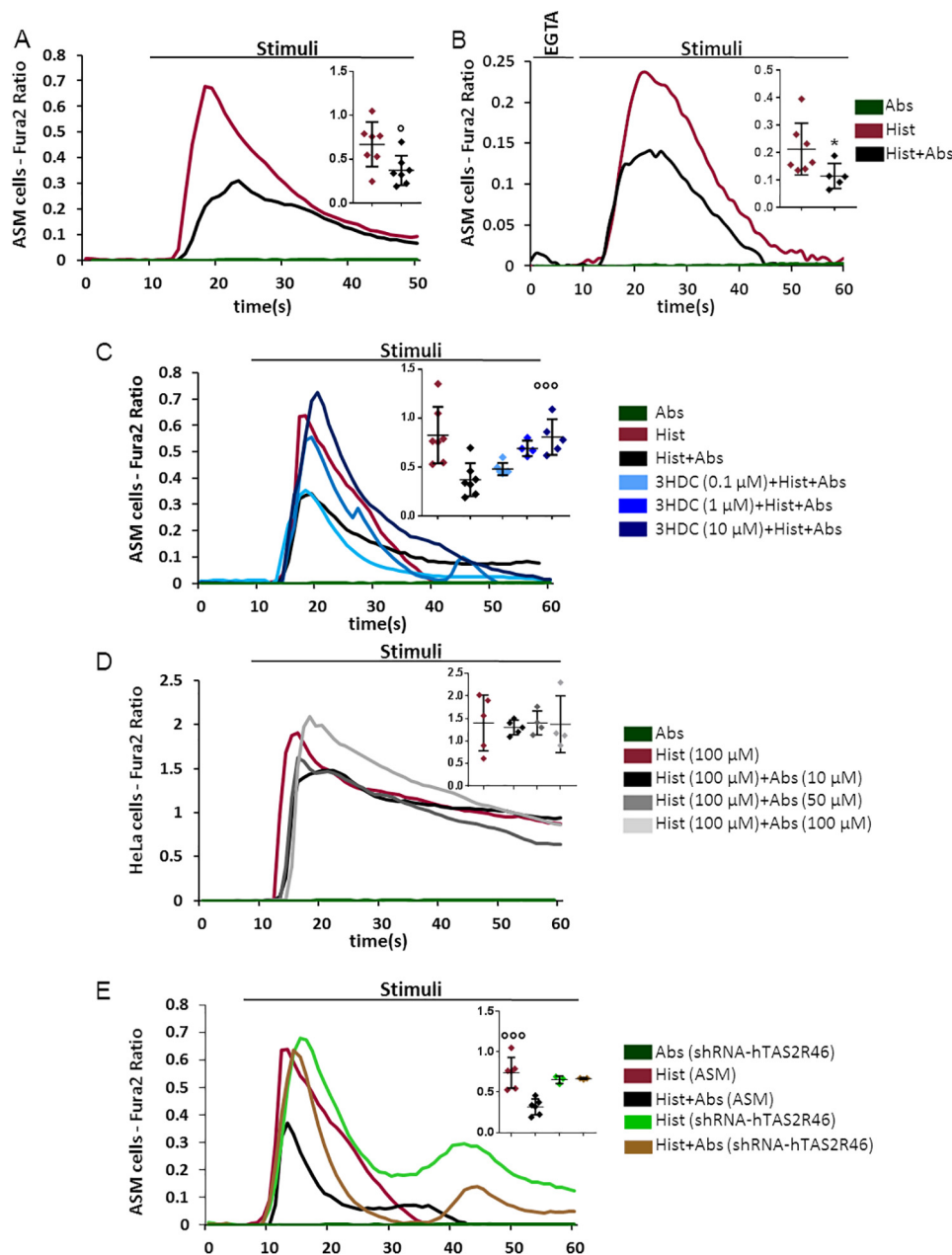


Figure 1. Absinthin reduces histamine-induced Ca^{2+} transients. Data are illustrated in representative traces as well as in scatter plots expressing the mean \pm S.D. of maximum peak of cytosolic Ca^{2+} release. *A* and *B*, fura-2-loaded ASM cells were stimulated with histamine (*Hist*) 10 μM and absinthin (*Abs*) 10 μM alone or combined, in the presence of calcium (*A*, Student's *t* test, $t_{(12)} = 2.57$, $t_{cr} = 2.17$; $^{\circ}$, $p = 0.024$) or in Ca^{2+} -free conditions (EGTA 100 μM) (*B*, Welch's *t* test, $t_{(9,13)} = 2.39$, $t_{cr} = 2.26$; * , $p = 0.040$). *C*, ASM cells stimulated with histamine (*Hist*, 10 μM), absinthin (*Abs*, 10 μM) and increasing concentrations of receptor antagonist 3HDC (0.1, 1, 10 μM). A linear regression confirmed a statistically significant increasing trend in cytosolic free calcium response determined by 3HDC ($F_{(1,20)} = 16.45$, $F_{cr} = 4.35$; $^{\circ\circ}$, $p = 6.17 \cdot 10^{-4}$), whereas no significant difference was found between Hist and 3HDC (10 μM) + Hist + Abs (Student's *t* test, $t_{(10)} = 0.13$, $t_{cr} = 2.23$, $p = 0.90$). *D*, cytosolic calcium release measurement in nonexpressing hTAS2R46 HeLa cells stimulated with histamine (*Hist*, 100 μM) and absinthin at the indicated concentrations. No significant relation emerged by linearly regressing cytosolic free calcium against increasing doses of *Abs* ($F_{(1,16)} = 0.009$, $F_{cr} = 4.49$, $p = 0.93$). *E*, ASM cells infected with LVs carrying shRNA-hTAS2R46 and treated as in *A*. Absinthin modulation of histamine-induced calcium release was analyzed in the two cellular models through a two-way ANOVA. The presence of a statistically significant interaction between the two factors ($F_{(1,14)} = 11.40$, $F_{cr} = 4.6$, $p = 0.0045$) reflects the simple main effects for which the significant decrease in cytosolic calcium following absinthin addition observed in ASM ($^{\circ\circ}$, $p = 7.01 \cdot 10^{-4}$) completely vanished when moving to ASM shRNA-hTAS2R46 model ($p = 0.62$).

(27) whereas the addition of absinthin alone had no effect. In striking contrast to the effect on cytosolic Ca^{2+} , the histamine-induced mitochondrial Ca^{2+} rise in the presence of absinthin was significantly greater compared with histamine alone (Fig. 3A).

The above data appeared to suggest that the reduced cytosolic Ca^{2+} rise is paralleled by a paradoxical increase in mito-

chondrial Ca^{2+} uptake, *i.e.* it would suggest that histamine-induced Ca^{2+} release is unaffected by absinthin, but the Ca^{2+} is channeled to the mitochondria and not to the cytosol. If this were the case, it would be expected that disrupting the mitochondrial membrane potential, which drives Ca^{2+} uptake by the mitochondrial calcium uniporter (MCU), with FCCP, and thereby not permitting mitochondrial Ca^{2+}

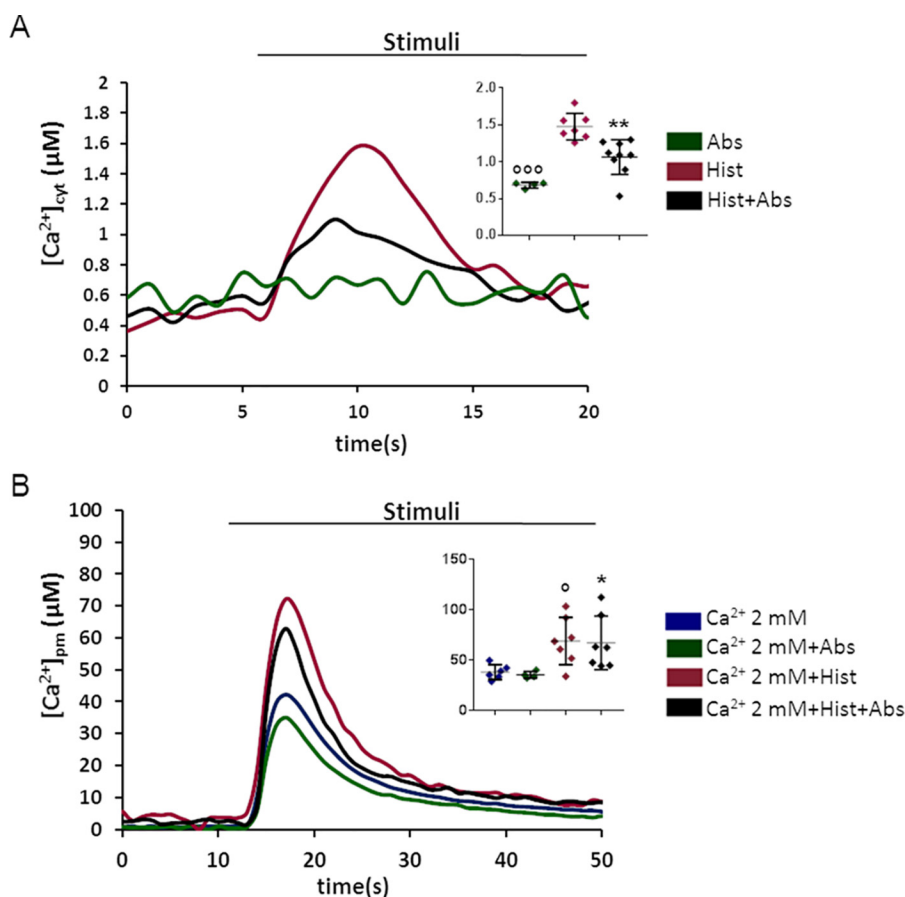


Figure 2. Absinthin does not affect subplasma membrane histamine-induced calcium transients. *A*, cytosolic Ca^{2+} variations in ASM cells infected with LV expressing cytAEQ after treatment with histamine (*Hist*, 10 μM) and/or absinthin (*Abs*, 10 μM) alone, or in combination. One-way ANOVA ($F_{(2,17)} = 22.04$, $F_{cr} = 3.59$, $p = 1.9 \cdot 10^{-5}$) with Dunnett's multiple comparison test versus Hist, ooo , $p = 1.6 \cdot 10^{-5}$; ** , $p = 0.0016$. *B*, subplasma membrane Ca^{2+} variations in ASM cells infected with LV expressing pmAEQ. Kruskal-Wallis *H* test ($H_{(3)} = 12.94$, $H_{cr} = 7.81$, $p = 0.0048$) with Dunn's multiple comparison test: Hist versus Ca^{2+} 2 mM $^{\circ}$, $p < 0.012$; Hist+Abs versus Ca^{2+} 2 mM * , $p = 0.015$; Hist+Abs versus Hist $p = 0.94$. Data are illustrated in representative traces as well as in scatter plots expressing the mean \pm S.D. of maximum peak of Ca^{2+} release.

uptake, should block the Ca^{2+} increase in mitochondria induced by histamine in the presence of absinthin and simultaneously restore the histamine- Ca^{2+} rise in the cytosol. Indeed, when FCCP was used, this resulted in a significantly reduced Ca^{2+} rise in mitochondria (Fig. 3A) and an increase in the cytosolic Ca^{2+} rise that was equivalent, if not greater, to histamine alone (Fig. 3B). Subplasmalemmal Ca^{2+} , on the contrary, was unchanged, suggesting that the extent of mitochondrial uptake does not influence Ca^{2+} entry via the plasma membrane (Fig. 3C).

Ca^{2+} -uptake in mitochondria is mediated by MCU, a protein complex whose main components have been recently identified (28, 29). In the presence of KB-R7943, a nonspecific inhibitor of the uniporter (30), the effect of absinthin on histamine-induced mitochondrial Ca^{2+} rises was abolished (Fig. 3A), as was the effect on cytosolic Ca^{2+} (Fig. 3B), whereas again no difference was perceivable in subplasmalemmal Ca^{2+} (Fig. 3C). FCCP or KB-R7943 alone did not affect basal Ca^{2+} or Ca^{2+} signals induced by histamine (Fig. S3, A–D).

An intact cytoskeletal structure is necessary for the action of absinthin

The above data would suggest that absinthin signals to the mitochondria to increase the uptake of the Ca^{2+} released from

the endoplasmic reticulum (ER). If this were the case, it could be expected that disrupting the ER-mitochondria juxtapositions would, at least in part, abolish the effect of absinthin. To this extent, we pre-incubated cells with latrunculin, a natural compound that disrupts the actin cytoskeleton thereby uncoupling organelle cross talk (31). As observed in Fig. 4A, in cells pre-incubated with latrunculin, the cytosolic Ca^{2+} rises induced by histamine were similar in the presence or absence of absinthin in the cytosol (Fig. 4A; see Fig. 1 for traces in the absence of absinthin) under the plasma membrane (Fig. 4B) and in mitochondria (Fig. 4C).

Neither a change in mitochondrial membrane potential nor a change in ATP/ADP ratio occurs upon absinthin addition

We reasoned that absinthin might modify the mitochondrial potential, and this might then be responsible for the increased mitochondrial accumulation. To test for this, we used the JC-1 probe, but found no difference of mitochondrial membrane potential in the presence or absence of absinthin (Fig. S4A).

Next, we investigated whether an increase in mitochondrial Ca^{2+} during this time frame could significantly increase cytosolic ATP levels. If this were the case, it could be expected that extruding mechanisms could be more efficient and it could

hTAS2R46 regulates mitochondrial calcium buffering

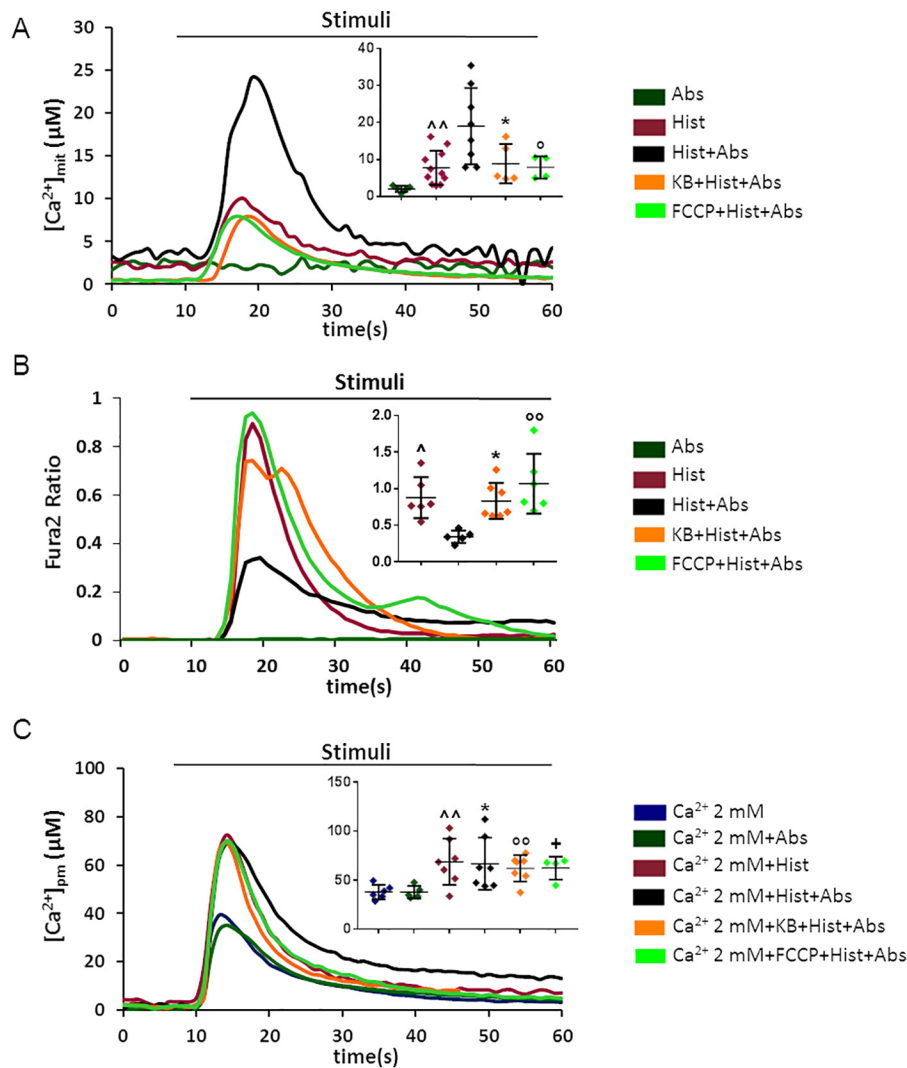


Figure 3. Absinthin potentiates mitochondrial histamine-induced calcium transients. *A*, mitochondrial calcium concentrations in ASM cells infected with LV expressing mitAEQ after treatment with histamine (*Hist*, 10 μM), absinthin (*Abs*, 10 μM), KB-R7943 (10 μM), FCCP (10 μM). One-way ANOVA ($F_{(3,24)} = 5.02$, $F_{cr} = 3.00$, $p = 0.0076$) with Dunnett's multiple comparison test *versus* Hist+Abs, \wedge , $p = 0.0022$; *, $p = 0.038$; \circ , $p = 0.033$. *B*, cytosolic Ca^{2+} changes using identical conditions to (*A*) but determined by Fura-2. One-way ANOVA ($F_{(3,20)} = 6.23$, $F_{cr} = 3.10$, $p = 0.0037$) with Tukey's multiple comparison test: Hist *versus* Hist+Abs \wedge , $p = 0.027$; KB+Hist+Abs *versus* Hist+Abs *, $p = 0.039$; FCCP+Hist+Abs *versus* Hist+Abs \circ , $p = 0.0023$; KB+Hist+Abs *versus* Hist $p = 0.99$; FCCP+Hist+Abs *versus* Hist $p = 0.65$. *C*, subplasma membrane Ca^{2+} variations using identical conditions to (*A*). Kruskal-Wallis *H* test ($H_{(5)} = 16.42$, $H_{cr} = 11.07$, $p = 0.0057$) with Dunn's multiple comparison test: all *versus* Ca^{2+} 2 mM, \wedge , $p = 0.0059$; *, $p = 0.016$; \circ , $p = 0.008$; \dagger , $p = 0.027$. All the comparisons involving KB+Hist+Abs or FCCP+Hist+Abs *versus* both Hist and Hist+Abs did not show statistically significant differences ($p \geq 0.82$). Data are illustrated in representative traces as well as in scatter plots expressing the mean \pm S.D. of maximum peak of Ca^{2+} release.

account for part of the drop in cytosolic Ca^{2+} . As shown in Fig. 5A, absinthin, unlike the positive control FCCP, was unable to modify significantly ATP to ADP ratios.

β_2 -adrenoreceptor activation mimics the effects of hTAS2R46 activation

To evaluate whether other plasma membrane receptor agonists were able to trigger a similar mechanism, we investigated the Ca^{2+} response of histamine in the presence of a β_2 agonist, the most widely used bronchodilators in asthma and chronic obstructive pulmonary disease. As expected, salbutamol (10 μM) lowered the Ca^{2+} rise induced by histamine (Fig. 5A). This has been reported previously and has been attributed to a number of cAMP- and PKA-dependent effects, including IP_3 receptor modulation (32). Surprisingly, though, histamine-induced

mitochondrial Ca^{2+} increased significantly also in the presence of salbutamol (Fig. 5A).

cAMP or EPAC modulation modifies cytosolic and mitochondrial histamine-induced Ca^{2+} transients in HeLa and ASM cells

Given that β_2 receptors are coupled to cAMP formation, we attempted to reproduce the effect with forskolin (10 μM). In the presence of forskolin, cytosolic histamine-induced Ca^{2+} rises were significantly blunted (Fig. 5A). When evaluating mitochondrial calcium, the concentration was also blunted, although not to the same extent (Fig. 5A). Yet, the effect of a strong cAMP production induced by forskolin prevented firm conclusions.

From the data on forskolin and, more importantly on salbutamol, it would appear that a cAMP-dependent pathway may

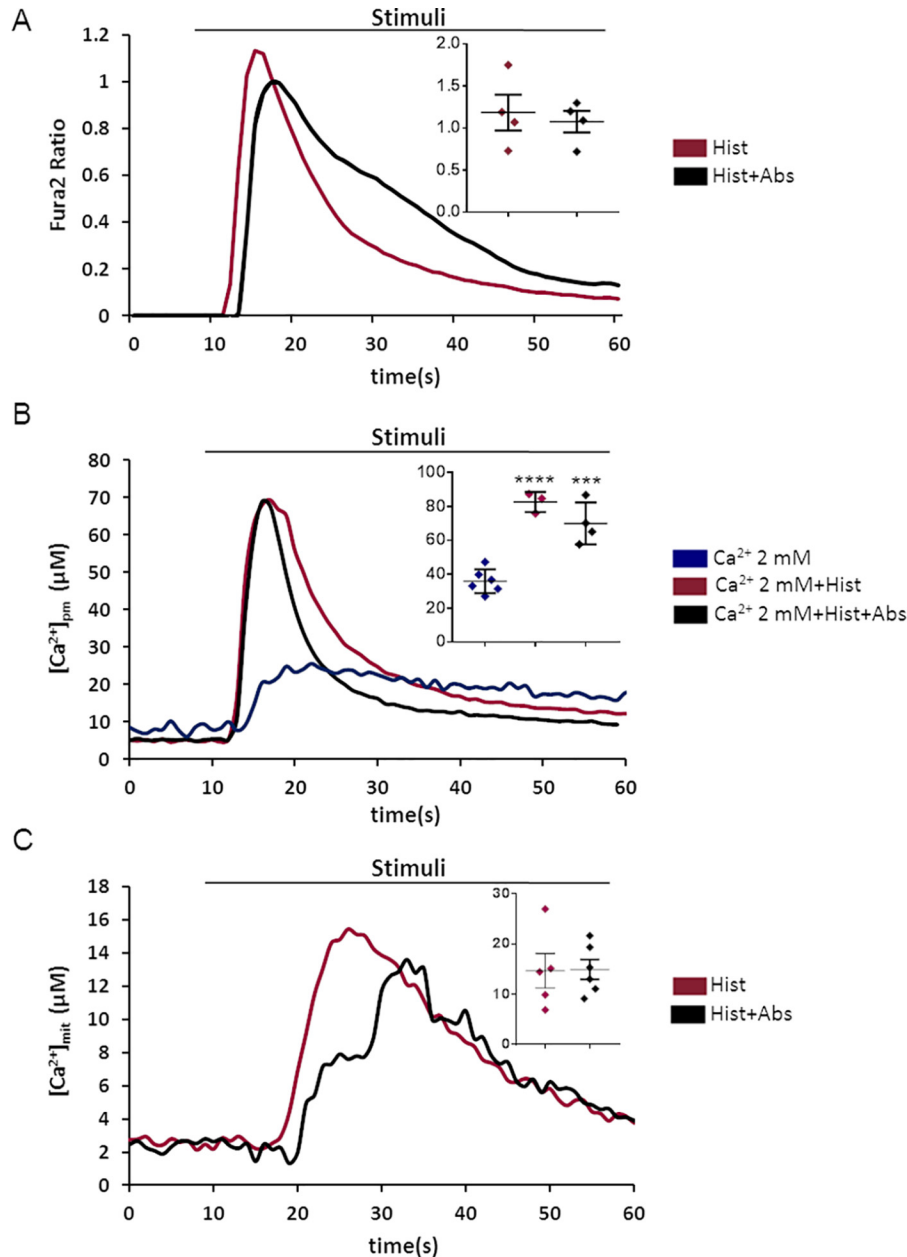


Figure 4. Effect of actin filament disruption on absinthin modulation of histamine-induced Ca²⁺ transients. *A*, fura-2-loaded ASM cells were stimulated with histamine (*Hist*) 10 µM with or without absinthin (*Abs*) 10 µM in the presence of latrunculin A (10 µM for 1 h). Student's *t* test, $t_{(6)} = 0.44$, $t_{cr} = 2.45$, $p = 0.68$. *B*, subplasma membrane Ca²⁺ variations using identical conditions to (*A*). One-way ANOVA ($F_{(2,10)} = 34.06$, $F_{cr} = 4.10$, $p = 3.44 \cdot 10^{-5}$) with Tukey's multiple comparison test: *Hist* versus Ca²⁺ 2 mM ****, $p = 5.66 \cdot 10^{-5}$; *Hist*+ *Abs* versus Ca²⁺ 2 mM ***, $p = 0.0004$; *Hist* versus *Hist*+ *Abs* $p = 0.19$. *C*, mitochondrial calcium concentrations using identical conditions to (*A*). Student's *t* test, $t_{(9)} = 0.067$, $t_{cr} = 2.26$, $p = 0.95$. Data are illustrated in representative traces as well as in scatter plots expressing the mean ± S.D. of maximum peak of Ca²⁺ release.

control ER to mitochondria Ca²⁺ shuttling. It has been recently reported that Epac1 is localized on the mitochondrial inner membrane and matrix (and may control MCU activity) (33, 34). To test whether the actions of absinthin were mediated by EPAC, we performed identical experiments to those described using the EPAC-specific inhibitor ESI-09. As shown in Fig. 5B, ESI-09 was able to counteract the effect of absinthin on both cytosolic and mitochondrial Ca²⁺.

We next proceeded to investigate cAMP rises upon histamine, histamine/absinthin, and forskolin in ASM cells using a cytosolic FRET probe. As expected, forskolin induced a rise in

cytosolic cAMP in the same time frame as the regulation of histamine-induced Ca²⁺ rises. On the contrary, however, absinthin did not appear to have any direct effect on cAMP levels in this time frame (Fig. S5).

Last, we investigated whether the same effect was observable in another cell type, HeLa. As shown in Fig. 5C both forskolin and the EPAC activator 8-pCPT-2'-O-Me-cAMP were able to reduce cytosolic Ca²⁺ rises induced by histamine while increasing mitochondrial Ca²⁺ rises, confirming that the phenomenon is likely to be present in other cell types.

We believe this is the first report of a positive modulation of mitochondrial Ca^{2+} uptake by plasma membrane G protein-coupled receptors, although it had been long known that receptor agonists are able to increase mitochondrial Ca^{2+} (35) and that postulations on the role of mitochondrial uptake in shaping cytosolic signals date back in time (36). Indeed, one of the most striking characteristics of this modulation is the speediness by which it occurs, as simultaneous activation of histamine receptors and TAS2R46/ β_2 -adrenoreceptors is sufficient to elicit an effect. When superimposing traces, the mitochondrial Ca^{2+} transient lags just a few seconds behind the cytosolic transient.

Although it is possible that TAS2R46 activation directly affects the signaling of histamine receptors (for example reducing the Gq coupling), this would explain the reduction in cytosolic Ca^{2+} but would be unable to explain the increase in mitochondrial Ca^{2+} and the absence of a difference in subplasmalemmal Ca^{2+} .

It is thought that microdomains of high Ca^{2+} at the mouth of IP_3 receptors are necessary in ER-mitochondria juxtapositions to drive Ca^{2+} uptake into mitochondria. Ca^{2+} flows through the voltage-dependent anion channel (VDAC), located on the mitochondrial outer membrane, and then through the mitochondrial Ca^{2+} uniporter located on the inner membrane. Importantly, a Ca^{2+} increase in mitochondria has physiological repercussions, including an increased activity of pivotal oxidative phosphorylation enzymes (37) and a protection from excessive Ca^{2+} surges. It has been recently suggested that Epac1 favors Ca^{2+} exchange between the ER and the mitochondrion in heart via the VDAC/GRP75/ $\text{IP}_3\text{R1}$ complex (34), and it is likely that a similar mechanism occurs in smooth muscle cells.

In this respect, it can be imagined that TAS2R46 activation not only controls histamine-induced Ca^{2+} contractions but also provides an energetic boost to smooth muscle cells and protects them. Indeed, genetic ablation or inhibition of EPAC1 in cardiac myocytes has been shown as protective in myocardial ischemia/reperfusion injury (33). In this respect, it is interesting to note that a TAS2R ligand has been recently reported to decrease mitochondrial membrane potential and increase mitochondrial reactive oxygen species and mitochondrial fragmentation (38). Yet, when we tested membrane potential changes with absinthin, we were unable to detect any. Furthermore, an energetic boost stimulated by Ca^{2+} (39) should be expected to increase ATP to ADP ratio in the cytosol (which in turn could also render Ca^{2+} pumps more efficient and partly explain the cytosolic drop). Yet, by using a PercevalHR probe, which measures ATP/ADP ratios (see [supporting Experimental procedures](#)), we were unable to detect any significant changes in the time frame of treatment. The possibility that ATP/ADP ratios were below our threshold of detection is possible.

Although we have not investigated the molecular mechanism of action of the Ca^{2+} shuttling, a few hypotheses can be made. First, TAS2R46 could be controlling ER-mitochondria juxtapositions, a mechanism that has been postulated by others to modify mitochondrial uptake (40–42). In this respect, when we performed time-lapse microscopy using MitoTracker, we were

unable to see any significant movements of mitochondria during the 100 s post treatment (data not shown). Alternatively, a posttranslational event could occur either on VDAC/MCU or one of its regulatory proteins (e.g. MICU, mitofusin). VDAC is known to increase its conductance for Ca^{2+} in its closed conformation (43) and such an event could explain the increased amount of Ca^{2+} entering the mitochondria. A regulation of MCU is also possible, although its localization on the inner membrane would create a topological problem, it should be noticed that the regulation is rapid, as simultaneous addition of histamine and absinthin/salbutamol is sufficient to unmask the effect.

Independently of the mechanism by which this occurs, we believe we have shown that activation of TAS2R46 leads to a redirection of IP_3R Ca^{2+} efflux from the cytosol to the mitochondria (i.e. from cytosolic modulation to mitochondrial regulation), and this is most likely mediated by EPAC, providing a further mechanism by which Ca^{2+} signals can be encoded by cells.

A limitation of our study was our inability to detect cAMP rises upon absinthin addition. This may suggest that our FRET system does not have sufficient spatial resolution to detect discrete microdomains of cAMP (44), that the size of the cAMP increase is below the limit of detection, or that cAMP increases in mitochondria and not in the cytosol. This last hypothesis would be supported by a recent paper that showed that aldosterone increases selectively the activity of the soluble adenylyl cyclase in the mitochondria and that the inhibition of EPAC reduced mitochondrial Ca^{2+} uptake, in a similar fashion to what was observed in the present contribution (45). It would be unlikely that EPAC, instead, is activated in a cAMP-independent fashion as this has never been reported previously. What links TAS2R46 to EPAC is therefore so far elusive.

It is generally accepted that high concentrations of cAMP, via PKA, are able to potentiate IP_3 -induced Ca^{2+} release via phosphorylation of the IP_3 receptor (Ref. 46 and references therein). Our study does not contradict such notion as we have always used maximal concentrations of histamine whereas submaximal concentrations of phospholipase C-coupled receptor agonists are required to see this potentiation. Furthermore, we could not detect significant cAMP rises in the cytosol and it is therefore unlikely that a cytosolic PKA is activated in our conditions.

Recently, Dale *et al.* (47) have shown that in human bronchial airway smooth muscle cells, histamine-induced cytosolic Ca^{2+} rises may be blunted by isoproterenol and proposed a model by which compartmentalized cAMP rises negatively feedback via PKA to the histamine receptor. In our study, we were unable to determine the absolute level of Ca^{2+} released and therefore cannot rule out that IP_3 formation from histamine activation is reduced upon TAS2R46 activation. It is therefore possible that the two events occur simultaneously. Interestingly, Dale *et al.* (47) are able to observe an effect on histamine but not on other Ca^{2+} -mobilizing agents, suggesting a certain degree of specificity. Preliminary data from our lab also shows that the mito-

hTAS2R46 regulates mitochondrial calcium buffering

chondrial uptake increase is not evident when carbachol or bradykinin are used to induce Ca^{2+} mobilization.⁵

It should be noted that we used a single Ca^{2+} indicator for mitochondria (aequorin). Although it is unlikely that this may have resulted in artifacts, given also the consistency of results across protocols, this limitation should be acknowledged.

To describe this new Ca^{2+} -signaling pathway, we made use of fluorescent imaging, a common technique in the field, coupled to aequorin-targeted probes and luminometry, which are less frequently employed. For these reasons, it might not be surprising that we have also unraveled a new mechanism that mediates the effect of β_2 -agonists, among the most studied receptors in pharmacology.

Experimental procedures

Absinthin isolation

A voucher specimen of the Pancalieri chemotype of *Artemisia absinthium* is kept in Novara laboratories. 1300 g of leaves and flowers, powdered, were extracted with acetone (3×7.5 liters) in a vertical percolator at room temperature, affording 97 g (7.5%) of a dark green syrup. The acetonic extract was dissolved into the minimal amount of acetone at 45 °C and then 97 g silica gel was added (ratio extract/silica 1:1); finally the suspension was evaporated. The powder obtained in this way was stratified on a layer of 485 g of aluminum oxide (ratio extract/alumina 1:5) packed with petroleum ether (40:60) and protected on its surface by a filter paper in a sintered filtration funnel (9×15 cm) with side arm for vacuum. The dissolved extract was purified with petroleum ether–ethyl acetate gradient from 90:10 to 60:40 (100 ml fraction) by vacuum chromatography. Fractions eluted with petroleum ether–ethyl acetate 40:60 afforded 8.7 g of pure absinthin (0.66%) whose structure elucidation and purity were confirmed from ¹H NMR (Fig. S6) according to Beauhaire *et al.* (48).

Cell culture

Human primary lung ASM cells were obtained from ATCC (catalog PCS-130-010). ASM cells were maintained in Vascular Cell Basal Medium (ATCC, catalog PCS-100-030) supplemented with 5% heat-inactivated fetal bovine serum (FBS), 5% L-glutamine, 0.5% antibiotic-antimycotic (all Thermo Fisher), 5 ng/ml of basic fibroblasts growth factor and 5 ng/ml epidermal growth factor (ImmunoTools), 50 $\mu\text{g}/\text{ml}$ of ascorbic acid, 10 ng/ml of insulin (Sigma-Aldrich).

HEK293T and HeLa cells were maintained in DMEM (Sigma-Aldrich) supplemented with 10% FBS, 1% L-glutamine, and 1% antibiotic-antimycotic.

Lentiviral vectors (LVs) for hTAS2R46 shRNA

hTAS2R46 was silenced by lentiviral infection. Several lentiviral constructs targeting hTAS2R46 were obtained from TRC-Hs1.0 library (Dharmacon). Third-generation LVs were produced co-transfecting HEK293T packaging cells with plasmids pMDLg/pRRE, pMD2.VSVG, pRSV-Rev and transfer construct using the Lipofectamine (Life Technologies) transfection

method and concentrated by PEG precipitation, as described previously (24). ASM cells were infected with the two LV-shRNAs (TCRN0000014110 and TCRN0000014112) together (referred as to shRNA-hTAS2R46) and the silencing was assessed by real time PCR and Western blotting as described in the [supporting information](#).

Calcium imaging

5×10^4 ASM or HeLa cells were plated on glass coverslips coated with poly-L-lysine (Sigma). The next day cells were loaded with Fura-2AM (5 μM) and pluronic acid (0.005%) (all Thermo Fisher) in Vascular Cell Basal Medium for 30 min at room temperature in the dark. After washing and de-esterification (20 min) the coverslip was mounted in a chamber equipped with a thermostat and placed on the stage of a Leica epifluorescence microscope equipped with a S Fluor 40 \times /1.3 objective. Cells were alternatively excited at 340/380 nm by the monochromator Polichrome V (Till Photonics, Munich, Germany) and the fluorescent signal was collected by a CCD camera (Hamamatsu, Japan) through band-pass 510 nm filter; the experiments were controlled and images analyzed with MetaFluor (Molecular Devices, Sunnyvale, CA) software. The cells were treated with the following stimuli alone or combined: histamine 10 μM (Sigma-Aldrich); absinthin 10 μM ; KB-R7943 (Sigma-Aldrich) 10 μM ; FCCP (Sigma-Aldrich); 3HDC (7) 0.1, 1, and 10 μM ; salbutamol 10 μM (Sigma-Aldrich); and forskolin 10 μM (Sigma-Aldrich). To quantify the differences in the peaks of Ca^{2+} transients the ratio values were normalized using the formula $(F_o - F_c)/F_o$ (referred to as normalized Fura-2 ratio; norm. ratio). To evaluate absinthin effect in calcium-free conditions, cytosolic Ca^{2+} was monitored upon depletion of external Ca^{2+} (by EGTA 100 μM). Actin filament disrupter latrunculin A was used at 10 μM (Sigma-Aldrich).

Aequorin-based Ca^{2+} measurements

We have monitored fluctuations of Ca^{2+} concentrations in the cytosol, in the domains adjacent to the plasma membrane, and in the mitochondrial matrix. To this end, we have used third-generation LVs to infect cells with the constructs encoding the native aequorin (cytAEQ-LV) or aequorin N-terminally linked to the synaptic-associated protein 25 (SNAP-25) (pLV-pmAEQ-LV) or to the COXVIII cleavable leader sequence (mitAEQ-LV). Generation of the plasmids was reported elsewhere (24). Lentiviral particles were produced by Lipofectamine transfection of HEK293T cells and concentrated by PEG precipitation (24). To monitor Ca^{2+} levels in different cellular compartments we used a custom built aequorinometer (CAIRN Research). ASM and HeLa cells were plated on 12 mm coverslips in a 24-well plate at a density 2×10^4 cells/well. After 24 h, cells were infected with cytAEQ-, pmAEQ-, or mitAEQ-expressing lentiviral particles. After 48–72 h, cells were washed with Krebs-Ringer buffer (KRB; 135 mM NaCl, 5 mM KCl, 0.4 mM KH_2PO_4 , 1 mM MgSO_4 , 5.5 mM glucose, 20 mM HEPES, pH 7.2) and reconstituted with native coelenterazine (catalog C2230, Sigma-Aldrich) at 37 °C, in dark for 30 min. Then, coverslips were transferred into perfusion chamber of the aequorinometer. To assess subplasma membrane calcium, cells were firstly perfused with KRB containing 100 μM EGTA for 100 s for

⁵ M. Talmon and L. Fresu, unpublished results.

baseline recording, and then the perfusion solution was switched to KRB-EGTA 100 μM supplemented with 20 μM *t*BHQ (Sigma-Aldrich). After 120 s cells were perfused with KRB- Ca^{2+} 2 mM in presence of the stimuli of interest alone or combined: histamine 10 μM , absinthin 10 μM , salbutamol 10 μM , KB-R7943 10 μM , FCCP 10 μM , forskolin 10 μM . To assess calcium changes in the cytosol or mitochondria, cells were perfused with KRB containing Ca^{2+} 2 mM for 100 s and then with KRB- Ca^{2+} added by the already mentioned stimuli. HeLa cells were also challenged with histamine in presence of 8-pCPT-2'-*O*-Me-cAMP (10 μM ; Sigma-Aldrich) a cAMP analogue that specifically activates EPAC (49). For quantification of Ca^{2+} concentration, at the end of each experiment cells were perfused with distilled water containing 0.1% Triton and 50 mM Ca^{2+} to discharge the remaining aequorin pool. Emitted light was converted in Ca^{2+} concentrations offline using a previously described algorithm (50). All measurements were carried out at 37 °C.

Statistical analysis

Data are presented as mean \pm S.D. of *n* independent experiments. All samples were first tested for normality (Shapiro-Wilk test) and for homogeneity of variance (Levene's test). When possible, statistical significance was assessed by parametric tests, *i.e.* linear regression and *t* test or one-way analysis of variance (ANOVA) (followed by Tukey's or Dunnett's post hoc test) in the case of continuous and categorical independent variables, respectively. Otherwise, nonparametric alternatives were used, as detailed in the figure legends. Unless otherwise specified, all statistical tests were between unpaired samples, two-tailed, and a *p* value < 0.05 was considered statistically significant.

Author contributions—M. T., A. A. G., and L. G. F. conceptualization; M. T. and F. A. R. data curation; M. T., D. L., F. A. R., and L. G. F. formal analysis; M. T., S. R., F. P., G. P., P. M., and R. B. investigation; M. T., S. R., D. L., F. P., and P. M. methodology; M. T., A. A. G., and L. G. F. writing-review and editing; D. L. and A. A. G. supervision; P. M., A. A. G., and L. G. F. resources; A. A. G. and L. G. F. writing-original draft; A. A. G. project administration; L. G. F. funding acquisition.

Acknowledgment—We thank Beatrice Riva for invaluable assistance with calcium imaging experiments.

References

- Lush, I. E., Hornigold, N., King, P., and Stoye, J. P. (1995) The genetics of tasting in mice. VII. Glycine revisited, and the chromosomal location of Sac and Soa. *Genet. Res.* **66**, 167–174 [CrossRef Medline](#)
- Bachmanov, A. A., Inoue, M., Ji, H., Murata, Y., Tordoff, M. G., and Beauchamp, G. K. (2009) Glutamate taste and appetite in laboratory mice: Physiologic and genetic analyses. *Am. J. Clin. Nutr.* **90**, 756S–763S [CrossRef Medline](#)
- Adler, E., Hoon, M. A., Mueller, K. L., Chandrashekar, J., Ryba, N. J., and Zuker, C. S. (2000) A novel family of mammalian taste receptors. *Cell* **100**, 693–702 [CrossRef Medline](#)
- Chandrashekar, J., Mueller, K. L., Hoon, M. A., Adler, E., Feng, L., Guo, W., Zuker, C. S., and Ryba, N. J. (2000) T2Rs function as bitter taste receptors. *Cell* **100**, 703–711 [CrossRef Medline](#)
- Meyerhof, W. (2005) Elucidation of mammalian bitter taste. *Rev. Physiol. Biochem. Pharmacol.* **154**, 37–72 [CrossRef Medline](#)
- Meyerhof, W., Batram, C., Kuhn, C., Brockhoff, A., Chudoba, E., Bufe, B., Appendino, G., and Behrens, M. (2010) The molecular receptive ranges of human TAS2R bitter taste receptors. *Chem. Senses* **35**, 157–170 [CrossRef Medline](#)
- Brockhoff, A., Behrens, M., Roudnitzky, N., Appendino, G., Avonto, C., and Meyerhof, W. (2011) Receptor agonism and antagonism of dietary bitter compounds. *J. Neurosci.* **31**, 14775–14782 [CrossRef Medline](#)
- An, S. S., and Liggett, S. B. (2018) Taste and smell GPCRs in the lung: Evidence for a previously unrecognized widespread chemosensory system. *Cell. Signal.* **41**, 82–88 [CrossRef Medline](#)
- Behrens, M., and Meyerhof, W. (2011) Gustatory and extragustatory functions of mammalian taste receptors. *Physiol. Behav.* **105**, 4–13 [CrossRef Medline](#)
- Deshpande, D. A., Robinett, K. S., Wang, W. C., Sham, J. S., An, S. S., and Liggett, S. B. (2011) Bronchodilator activity of bitter tastants in human tissue. *Nat. Med.* **17**, 776–778 [CrossRef Medline](#)
- Deshpande, D. A., Wang, W. C., McIlmoyle, E. L., Robinett, K. S., Schilling, R. M., An, S. S., Sham, J. S., and Liggett, S. B. (2010) Bitter taste receptors on airway smooth muscle bronchodilate by localized calcium signaling and reverse obstruction. *Nat. Med.* **16**, 1299–1304 [CrossRef Medline](#)
- Grassin-Delyle, S., Abrial, C., Fayad-Kobeissi, S., Brollo, M., Faisy, C., Alvarez, J. C., Naline, E., and Devillier, P. (2013) The expression and relaxant effect of bitter taste receptors in human bronchi. *Respir. Res.* **14**, 134 [CrossRef Medline](#)
- Liggett, S. B. (2013) Bitter taste receptors on airway smooth muscle as targets for novel bronchodilators. *Expert Opin. Ther. Targets* **17**, 721–731 [CrossRef Medline](#)
- Robinett, K. S., Koziol-White, C. J., Akoluk, A., An, S. S., Panettieri, R. A., Jr., and Liggett, S. B. (2014) Bitter taste receptor function in asthmatic and nonasthmatic human airway smooth muscle cells. *Am. J. Respir. Cell Mol. Biol.* **50**, 678–683 [CrossRef Medline](#)
- Zhang, C. H., Lifshitz, L. M., Uy, K. F., Ikebe, M., Fogarty, K. E., and ZhuGe, R. (2013) The cellular and molecular basis of bitter tastant-induced bronchodilation. *PLoS Biol.* **11**, e1001501 [CrossRef Medline](#)
- Pulkkinen, V., Manson, M. L., S  fholm, J., Adner, M., and Dahl  n, S. E. (2012) The bitter taste receptor (TAS2R) agonists denatonium and chloroquine display distinct patterns of relaxation of the guinea pig trachea. *Am. J. Physiol. Lung Cell. Mol. Physiol.* **303**, L956–L966 [CrossRef Medline](#)
- Bai, Y., Krishnamoorthy, N., Patel, K. R., Rosas, I., Sanderson, M. J., and Ai, X. (2016) Cryopreserved human precision-cut lung slices as a bioassay for live tissue banking. A viability study of bronchodilation with bitter-taste receptor agonists. *Am. J. Respir. Cell Mol. Biol.* **54**, 656–663 [CrossRef Medline](#)
- Camoretti-Mercado, B., Pauer, S. H., Yong, H. M., Smith, D. C., Deshpande, D. A., An, S. S., and Liggett, S. B. (2015) Pleiotropic effects of bitter taste receptors on $[\text{Ca}^{2+}]_i$ mobilization, hyperpolarization, and relaxation of human airway smooth muscle cells. *PLoS One* **10**, e0131582 [CrossRef Medline](#)
- Tan, X., and Sanderson, M. J. (2014) Bitter tasting compounds dilate airways by inhibiting airway smooth muscle calcium oscillations and calcium sensitivity. *Br. J. Pharmacol.* **171**, 646–662 [CrossRef Medline](#)
- Brockhoff, A., Behrens, M., Massarotti, A., Appendino, G., and Meyerhof, W. (2007) Broad tuning of the human bitter taste receptor hTAS2R46 to various sesquiterpene lactones, clerodane and labdane diterpenoids, strychnine, and denatonium. *J. Agric. Food Chem.* **55**, 6236–6243 [CrossRef Medline](#)
- Brockhoff, A., Behrens, M., Niv, M. Y., and Meyerhof, W. (2010) Structural requirements of bitter taste receptor activation. *Proc. Natl. Acad. Sci. U.S.A.* **107**, 11110–11115 [CrossRef Medline](#)
- Sauv  r, R., Diarra, A., Chahine, M., Simoneau, C., Morier, N., and Roy, G. (1991) Ca^{2+} oscillations induced by histamine H1 receptor stimulation in HeLa cells: Fura-2 and patch clamp analysis. *Cell Calcium* **12**, 165–176 [CrossRef Medline](#)
- Brini, M., Pinton, P., Pozzan, T., and Rizzuto, R. (1999) Targeted recombinant aequorins: Tools for monitoring $[\text{Ca}^{2+}]_i$ in the various compartments of a living cell. *Microsc. Res. Tech.* **46**, 380–389 [CrossRef Medline](#)

hTAS2R46 regulates mitochondrial calcium buffering

24. Lim, D., Bertoli, A., Sorgato, M. C., and Moccia, F. (2016) Generation and usage of aequorin lentiviral vectors for Ca^{2+} measurement in sub-cellular compartments of hard-to-transfect cells. *Cell Calcium* **59**, 228–239 [CrossRef Medline](#)
25. Marsault, R., Murgia, M., Pozzan, T., and Rizzuto, R. (1997) Domains of high Ca^{2+} beneath the plasma membrane of living A7r5 cells. *EMBO J.* **16**, 1575–1581 [CrossRef Medline](#)
26. Rizzuto, R., Simpson, A. W., Brini, M., and Pozzan, T. (1992) Rapid changes of mitochondrial Ca^{2+} revealed by specifically targeted recombinant aequorin. *Nature* **358**, 325–327 [CrossRef Medline](#)
27. Paillard, M., Tubbs, E., Thiebaut, P. A., Gomez, L., Fauconnier, J., Da Silva, C. C., Teixeira, G., Mewton, N., Belaidi, E., Durand, A., Abrial, M., Lacampagne, A., Rieusset, J., and Ovize, M. (2013) Depressing mitochondria-reticulum interactions protects cardiomyocytes from lethal hypoxia-reoxygenation injury. *Circulation* **128**, 1555–1565 [CrossRef Medline](#)
28. De Stefani, D., Raffaello, A., Teardo, E., Szabò, I., and Rizzuto, R. (2011) A forty-kilodalton protein of the inner membrane is the mitochondrial calcium uniporter. *Nature* **476**, 336–340 [CrossRef Medline](#)
29. Mishra, J., Jhun, B. S., Hurst, S., O-Uchi, J., Csordás, G., and Sheu, S. S. (2017) The mitochondrial Ca^{2+} uniporter: Structure, function, and pharmacology. *Handb. Exp. Pharmacol.* **240**, 129–156 [CrossRef Medline](#)
30. Santo-Domingo, J., Vay, L., Hernández-Sanmiguel, E., Lobatón, C. D., Moreno, A., Montero, M., and Alvarez, J. (2007) The plasma membrane $\text{Na}^+/\text{Ca}^{2+}$ exchange inhibitor KB-R7943 is also a potent inhibitor of the mitochondrial Ca^{2+} uniporter. *Br. J. Pharmacol.* **151**, 647–654 [CrossRef Medline](#)
31. Marchi, S., Patergnani, S., and Pinton, P. (2014) The endoplasmic reticulum-mitochondria connection: One touch, multiple functions. *Biochim. Biophys. Acta* **1837**, 461–469 [CrossRef Medline](#)
32. Billington, C. K., Penn, R. B., and Hall, I. P. (2017) β_2 Agonists. *Handb. Exp. Pharmacol.* **237**, 23–40 [CrossRef Medline](#)
33. Fazal, L., Laudette, M., Paula-Gomes, S., Pons, S., Conte, C., Tortosa, F., Sicard, P., Sainte-Marie, Y., Bissierier, M., Lairez, O., Lucas, A., Roy, J., Ghaleh, B., Fauconnier, J., Mialet-Perez, J., and Lezoualc'h, F. (2017) Multifunctional mitochondrial Epac1 controls myocardial cell death. *Circ. Res.* **120**, 645–657 [CrossRef Medline](#)
34. Wang, Z., Liu, D., Varin, A., Nicolas, V., Courilleau, D., Mateo, P., Caubere, C., Rouet, P., Gomez, A. M., Vandecasteele, G., Fischmeister, R., and Brenner, C. (2016) A cardiac mitochondrial cAMP signaling pathway regulates calcium accumulation, permeability transition and cell death. *Cell Death Dis.* **7**, e2198 [CrossRef Medline](#)
35. Tsuboi, T., da Silva Xavier, G., Holz, G. G., Jouaville, L. S., Thomas, A. P., and Rutter, G. A. (2003) Glucagon-like peptide-1 mobilizes intracellular Ca^{2+} and stimulates mitochondrial ATP synthesis in pancreatic MIN6 beta-cells. *Biochem. J.* **369**, 287–299 [CrossRef Medline](#)
36. Parekh, A. B. (2003) Mitochondrial regulation of intracellular Ca^{2+} signaling: More than just simple Ca^{2+} buffers. *News Physiol. Sci.* **18**, 252–256 [Medline](#)
37. Devin, A., and Rigoulet, M. (2007) Mechanisms of mitochondrial response to variations in energy demand in eukaryotic cells. *Am. J. Physiol. Cell Physiol.* **292**, C52–C58 [CrossRef Medline](#)
38. Pan, S., Sharma, P., Shah, S. D., and Deshpande, D. A. (2017) Bitter taste receptor agonists alter mitochondrial function and induce autophagy in airway smooth muscle cells. *Am. J. Physiol. Lung Cell Mol. Physiol.* **313**, L154–L165 [CrossRef Medline](#)
39. Griffiths, E. J., and Rutter, G. A. (2009) Mitochondrial calcium as a key regulator of mitochondrial ATP production in mammalian cells. *Biochim. Biophys. Acta* **1787**, 1324–1333 [CrossRef Medline](#)
40. Cieri, D., Vicario, M., Giacomello, M., Vallese, F., Filadi, R., Wagner, T., Pozzan, T., Pizzo, P., Scorrano, L., Brini, M., and Cali, T. (2017) SPLICS: A split green fluorescent protein-based contact site sensor for narrow and wide heterotypic organelle juxtaposition. *Cell Death Differ.* **25**, 1131–1145 [CrossRef Medline](#)
41. Csordás, G., Renken, C., Várnai, P., Walter, L., Weaver, D., Buttle, K. F., Balla, T., Mannella, C. A., and Hajnóczky, G. (2006) Structural and functional features and significance of the physical linkage between ER and mitochondria. *J. Cell Biol.* **174**, 915–921 [CrossRef Medline](#)
42. He, X., Bi, X. Y., Lu, X. Z., Zhao, M., Yu, X. J., Sun, L., Xu, M., Wier, W. G., and Zang, W. J. (2015) Reduction of mitochondria-endoplasmic reticulum interactions by acetylcholine protects human umbilical vein endothelial cells from hypoxia/reoxygenation injury. *Arterioscler. Thromb. Vasc. Biol.* **35**, 1623–1634 [CrossRef Medline](#)
43. Colombini, M. (2016) The VDAC channel: Molecular basis for selectivity. *Biochim. Biophys. Acta* **1863**, 2498–2502 [CrossRef Medline](#)
44. Zaccolo, M., and Pozzan, T. (2002) Discrete microdomains with high concentration of cAMP in stimulated rat neonatal cardiac myocytes. *Science* **295**, 1711–1715 [CrossRef Medline](#)
45. Szanda, G., Wisniewski, É., Rajki, A., and Spät, A. (2018) Mitochondrial cAMP exerts positive feedback on mitochondrial Ca^{2+} uptake via the recruitment of Epac1. *J. Cell Sci.* **16**, 131 [CrossRef Medline](#)
46. Taylor, C. W. (2017) Regulation of IP_3 receptors by cyclic AMP. *Cell Calcium* **63**, 48–52 [CrossRef Medline](#)
47. Dale, P., Head, V., Dowling, M. R., and Taylor, C. W. (2018) Selective inhibition of histamine-evoked Ca^{2+} signals by compartmentalized cAMP in human bronchial airway smooth muscle cells. *Cell Calcium* **71**, 53–64 [CrossRef Medline](#)
48. Beauhaire, J., Fourreya, J. L., Vuilhorgnea, M., and Lallemand, J. Y. (1980) Dimeric sesquiterpene lactones: Structure of absinthin. *Tetrahedron Lett.* **21**, 3191–3194 [CrossRef](#)
49. Enserink, J. M., Christensen, A. E., de Rooij, J., van Triest, M., Schwede, F., Genieser, H. G., Døskeland, S. O., Blank, J. L., and Bos, J. L. (2002) A novel Epac-specific cAMP analogue demonstrates independent regulation of Rap1 and ERK. *Nat. Cell Biol.* **4**, 901–906 [CrossRef Medline](#)
50. Brini, M., Marsault, R., Bastianutto, C., Alvarez, J., Pozzan, T., and Rizzuto, R. (1995) Transfected aequorin in the measurement of cytosolic Ca^{2+} concentration ($[\text{Ca}^{2+}]_c$). A critical evaluation. *J. Biol. Chem.* **270**, 9896–9903 [CrossRef Medline](#)